

Enhancing chlorophyll stability by regulating charge transfer in chlorophyll self-aggregation

Fangwei Li^{1,2,3,4}, Zhaotian Yang^{2,3}, Suxia Shen^{2,3}, Ajibola Nihmot Ibrahim⁵, Zhenhao Wang⁶ and Yan Zhang^{1,2,3*}

¹ Sanya Institute of China Agricultural University, Sanya 572025, China

² College of Food Science and Nutritional Engineering, China Agricultural University, Beijing 100083, China

³ National Engineering Research Center for Fruit and Vegetable Processing, Ministry of Science and Technology, Beijing 100083, China

⁴ College of Food Science and Engineering, Ocean University of China, Qingdao 266003, China

⁵ Department of Food Science and Technology, Faculty of Agriculture, Federal University Wukari, Taraba State, Nigeria

⁶ College of Chemical Engineering, Beijing University of Chemical Technology, Beijing 100029, China

* Corresponding author, E-mail: zhangyan348@163.com

Abstract

Chlorophyll (Chl), a natural pigment with broad applications in food systems, faces challenges due to its instability under light exposure. This study explores the relationship between solvent polarity, charge transfer (CT) in Chl self-aggregation, and photostability enhancement. By adjusting ethanol/water ratios (10–100% ethanol), environmental polarity was modulated to investigate its impact on CT dynamics using fluorescence spectroscopy, conductivity analysis, and quantum chemistry calculations. Results demonstrated that higher solvent polarity significantly strengthened CT interactions between Chl molecules, primarily mediated by porphyrin rings, while the hydrophobic phytol tail influenced aggregate configurations and indirectly modulated CT pathways. Light stability tests revealed that Chl retention in high-polarity solvents (10%–40% ethanol) surpassed low-polarity groups (60%–90% ethanol) by 213.04% and 302.61% on days 4 and 8, respectively, highlighting the critical role of CT-driven aggregation in mitigating photodegradation. Quantum calculations further elucidated that phytol tail removal altered CT efficiency depending on porphyrin spacing: in 'sandwich' dimers, phytol absence enhanced CT, whereas in 'face-to-face' configurations, partial removal optimized electron redistribution. These findings underscore solvent polarity as a key regulator of CT-mediated aggregation, offering a mechanism to stabilize Chl through non-covalent interactions. The study advances the understanding of Chl aggregation mechanisms and proposes physical strategies, such as electric-field-induced CT modulation, to enhance the stability of photosensitive natural pigments in food processing and storage.

Citation: Li F, Yang Z, Shen S, Ibrahim AN, Wang Z, et al. 2025. Enhancing chlorophyll stability by regulating charge transfer in chlorophyll self-aggregation. *Food Innovation and Advances* 4(4): 454–460 <https://doi.org/10.48130/fia-0025-0039>

Introduction

As a natural plant product, chlorophyll (Chl) has continuously attracted the attention of food researchers in recent years. Among all the naturally occurring pigments, Chl is the most abundantly distributed and is one of the most popular natural colorants in the food industry^[1]. In light of the growing consumer demand for minimally altered food ingredients, it is critical to innovate processing methodologies that safeguard the structural integrity of Chl throughout food production^[2]. However, few studies have investigated Chl as a food nutrient and natural colorant^[3–5]. Fortunately, there have been numerous studies on the photosynthetic, degradation, and antioxidant effects of Chl^[6–8]. These studies provide a solid theoretical foundation for the application of natural Chl in food nutrition and processing. Natural Chl is highly susceptible to degradation when exposed to light, thermal energy, and acidic conditions, with photodegradation being the most significant factor contributing to its instability^[9,10]. Chl self-aggregation was proved to be able to improve its own stability, with natural molecular structure remaining^[11]. However, the effect and principle of this aggregation to improve Chl photostability is not clear yet.

The Chl aggregation is dominated by non-covalent bonds, including electrostatic interaction, dispersion attraction, and exchange repulsion. Current research believes that the first two are the main forces promoting Chl monomers to attract each other to form aggregates^[12]. However, as the main pigment involved in photosynthesis, the charge transfer (CT) function of Chl should be given more

attention in aggregation. The biomimetic application of chlorophyll in photoelectric conversion provides valuable references^[13,14]. Moreover, CT is directly related to light, the biggest factor influencing Chl stability^[12,15]. Therefore, it is speculated that CT is likely to be another important force affecting the aggregation process of Chl. However, there are almost no studies on the role of CT in the stability of Chl aggregates in food systems.

The aggregation of Chl *in vitro* is easily affected by the changes of solvent characteristics. When the solvent has a high polarity, it enhances the aggregation of Chl molecules^[10]. The change in solvent polarity is related to its permittivity. In the context of Chl aggregation interactions, CT processes appear to exhibit the strongest correlation with solvent permittivity^[16]. The change in solvent polarity is related to its dielectric constant. Among the interactions of Chl aggregation, CT is most likely closely related to the dielectric constant of the solvent. Moreover, the occurrence of CT is most likely related to the chromophore of the molecule, which is related to the color stability of Chl. Therefore, further exploration is necessary to understand the induction mechanism of CT interaction through solvent polarity adjustment and its impact on Chl aggregation.

Meanwhile, Chl aggregation caused by the change of solvent polarity was probably related to the polarity of Chl's own fragment. Chl has a hydrophilic porphyrin ring head and a hydrophobic phytol tail^[6]. The phenomenon that strong solvent polarity promoted the aggregation implied that the interaction of Chl hydrophobic groups was more conducive to the formation of aggregates than the

interaction of hydrophilic groups. This was consistent with the Chl dimer structure in the previous study. The two phytol tails were sandwiched between two porphyrin rings^[11]. Based on the above analysis, the impact of phytol tail on CT during chlorophyll aggregation deserves further exploration.

In prior research, through a comparative analysis of atomic force microscopy images of Chl with a structural model of Chl aggregates optimized via quantum chemical calculations, it was established that Chl dimers constitute a prevalent aggregate form in Chl solutions^[12]. Meanwhile, since the dimer is the smallest aggregation structural unit, it was selected as the model for the aggregation study. On the other hand, the fluorescence spectroscopic analysis of Chl aggregates has also demonstrated that the structural difference between Chl *a* and Chl *b* has a negligible effect on Chl aggregation^[12]. Therefore, in this study, Chl *a*, which is more distributed in fruits, vegetables, and algae than Chl *b*, was used as the target molecule, and its dimer was used as the research model^[12].

In this research, water-ethanol was selected as the solvent of Chl. The self-aggregation of Chl was induced by regulating the polarity of the solvent. The relationship among solvent polarity, Chl stability and CT was discussed. Through quantum chemistry calculations, an attempt was made to explain the change in CT caused by the solvent polarity change and the mechanism by which Chl self-aggregation improved stability. Meanwhile, the effect of phytol tail on CT in Chl aggregate had also been explored. It is hoped that the results can expand ideas for improving the stability of Chl during food processing and storage. It is hoped that contributions can be made to improving the stability of photosensitive natural food ingredients and expanding the application of physical technology for the protection of food ingredients.

Materials and methods

Experimental materials

The Chl used in this study had a purity of 86.6%. Additionally, the neutral alumina, ethanol, petroleum ether, acetone, and n-butanol were acquired from Sinopharm Chemical Reagent Co., Ltd (Shanghai, China.). All reagents were of analytical grade. The chromatography column used for Chl separation and purification was purchased from Shanghai Suke Industrial Co., Ltd (Shanghai, China).

Quantum chemistry calculations and wave function analysis

The geometric optimization of molecular structure, single-point energy calculation, and excited state calculation were all realized by Gaussian 16 (A.03)^[17]. Density functional theory (DFT) and time-dependent density functional theory (TD-DFT) methods were applied in this research. The geometric optimization was realized by using the B3LYP-D3 (BJ) function combined with the 6-311G (d, p) basis set^[18,19]. The SMD solvent model was used. The *eps* corresponding to 10%, 20%, 30%, 40%, 50%, 60%, 70%, 80%, 90%, and 100% ethanol solutions were 73.1, 67.7, 62.3, 56.9, 51.5, 46.1, 40.7, 35.3, 29.9, and 24.5, respectively. The *epsinf* took the square of the refractive index as an approximate value, which were 1.77715561, 1.78543044, 1.79372449, 1.80203776, 1.81037025, 1.81872196, 1.82709289, 1.83548304, 1.84389241, and 1.852321. There was no virtual frequency in the optimized structures. Single point energy calculations were realized by using M06-2X function combined with 6-311G (2d, p) basis set^[20]. Excited state calculations were realized by the CAM-B3LYP-D3(BJ) function combined with 6-311G (d, p) basis set^[21]. Inter-fragment charge transfer (IFCT) analysis and hole-electron analysis were performed by Multiwfn 3.8^[22]. Visual Molecular Dynamics (VMD) software was used to draw the molecular structure model and its isosurface map.

Extraction and purification of Chl

The spinach used in the experiment was purchased from the vegetable market of PR China Agricultural University. The stems and veins of fresh spinach were removed, and 200 g of them was put into a homogenizer. Then 600 mL of absolute ethanol-petroleum ether (v:v = 1:2) was added to the homogenizer, and the sample was homogenized to a uniform liquid. After homogenization, the samples were frozen and centrifuged at 4 °C and 8,000 × g for 10 min. The supernatant was then collected and filtered under suction. The resulting sample was transferred to a separatory funnel, and an equal volume of water was added. After shaking, the mixture was allowed to stand for liquid separation. The lower water phase was removed, while the upper oil phase was retained. This step was repeated twice. The sample was then dried with anhydrous sodium sulfate and filtered. It was rotary evaporated at 36 °C to obtain a crude chlorophyll extract. The crude Chl extract was passed through a chromatography column with neutral alumina. Petroleum ether-acetone (v:v = 9:1), petroleum ether-acetone (v:v = 7:3), and n-butanol-ethanol-water (v:v:v = 3:1:1) were used sequentially as eluents, and carotene, lutein and Chl were eluted. The eluted Chl fraction, with a purity of 86.6%, was collected and stored for subsequent use.

Determination of Chl content

The determination of Chl content was referred to the method of Aktas & Yildiz with minor modifications^[23]. After diluting, 200 µL of sample was added to a 96-well plate, and the absorbances at 645 and 663 nm were measured with a microplate reader (SpectraMax iD5, Molecular Devices, USA). All experiments were performed under shading. The contents of Chl were calculated by the following formula:

$$\text{Chl } a \text{ concentration (mg/L)} : C_a = 12.71 \times A_{663} - 2.59 \times A_{645} \quad (1)$$

$$\text{Chl } b \text{ concentration (mg/L)} : C_b = 22.88 \times A_{645} - 4.67 \times A_{663} \quad (2)$$

$$\text{Chl concentration (mg/L)} : C = C_a + C_b = 8.04 \times A_{663} + 20.29 \times A_{645} \quad (3)$$

Sample preparation

Ethanol-water solutions were prepared with a Chl concentration of 83.90 mg/L for ten groups. The proportions of ethanol in each group were 10%, 20%, 30%, 40%, 50%, 60%, 70%, 80%, 90%, and 100 %, respectively. The samples were maintained under continuous light exposure at room temperature for 8 d. Illumination processing was realized by 32 W LED lights with a color temperature of 6,000 to 6,500 k. The color change of the Chl samples was recorded.

Determination of fluorescence spectrum

The fluorescence measurement of the Chl solution was carried out with a microplate reader (SpectraMax iD5, Molecular Devices, USA). The measurement was referred to the method of Merzlyak, Melø and Naqvi with some modifications^[24]. The fluorescence emission spectrum between 550 and 850 nm was measured with exciting at 393 nm. All measurements were performed using 96-well plates at room temperature. The slit width of the microplate reader was 20 nm.

Determination of conductivity

A conductivity meter (FE30, METTLER TOLEDO, Switzerland) was used to measure the conductivity of the sample. A solution with 0.01 mol/L KCl was used as the calibration solution. After calibration, the electrode was put into the sample, and measurement was performed. The conductivity value on the display was recorded.

Statistical analysis

The experimental data was expressed as 'average ± standard deviation', and the analysis of variance (ANOVA) of SPSS statistics

21 was used to analyze the significance of the experimental data. The significance level p was 0.05, and $p < 0.05$ indicated that the difference was significant. Origin 2018 was used for drawing graphs.

Results and discussion

The effect of solvent polarity on CT in Chl aggregates

The three factors that may affect CT in Chl aggregates include CT media, molecular groups, and the distance between donor and acceptor. Among them, studies have shown that CT was significantly affected by the distance between the donor and acceptor^[25]. As the distance increases, its strength will diminish. However, there were still few studies on the relationship among CT media, molecular fragments and CT strength.

The previous research confirmed that the Chl 'sandwich' dimer was a stable aggregate configuration^[11,12]. Therefore, the 'sandwich' dimer was employed in a vacuum as a model to investigate the impact of the phytol tail on charge transfer without the influence of a solvent. This 'sandwich' dimer in vacuum had a HOMO-LUMO orbital with significant CT characteristics, as shown in [Supplementary Fig. S1](#). The presence or absence of phytol tail had no significant effect on the CT characteristics of the dimer's HOMO-LUMO orbital. Therefore, the dimer model, which is easy to study the CT interaction between porphyrin rings, is more suitable for exploring the relationship between CT interaction and Chl aggregation in this study. After optimization by ab initio molecular dynamics, the 'face-to-face' dimer configuration of Chl was obtained, with the phytol tails oriented outward ([Fig. 1](#)). This was done to minimize the impact of the phytol tails on the configuration and allow for better control of the variable related to the phytol tails. This approach was beneficial in exploring the correlation between solvent changes and CT. Meanwhile, it was pointed out that the Chl 'face-to-face' dimer was also a stable Chl aggregate configuration^[11,12]. The selected fragments of the model are shown in ([Fig. 1](#)). Fragments 1 and 3 are porphyrin rings, while fragments 2 and 4 are phytol tails.

As a kind of thought experiment, under the condition that the configuration of the Chl dimers remained exactly the same, only the parameters of the solvent model were adjusted. The CT amounts of

different fragments in Chl dimer in ethanol with different concentrations were obtained, as shown in [Table 1](#). Different ethanol concentrations represented different polarities. When the proportion of ethanol was 10%, the polarity was the strongest, while the polarity was the weakest when the ethanol proportion was 100%. The fragments 1 and 2 were situated on one Chl molecule, while the fragments 3 and 4 were located on another. The degree of CT between the two porphyrin rings underwent significant changes as the polarity of the solvent varied. The levels of CT between the other fragments remained relatively low or even non-existent and did not change with the variation in solvent polarity. As a result, the overall level of CT in the Chl dimer also fluctuated with shifts in solvent polarity. Both the CT between the porphyrin rings and within the entire dimer exhibited a tendency to increase as the solvent polarity increased. High-polarity solvents possess enhanced molecular dipole moments, enabling effective stabilization of charge-separated states through solvation effects. During charge transfer processes, these solvent molecules facilitate the stabilization of the resulting ion pairs, thereby reducing the system's overall free energy. Furthermore, high-polarity solvents typically exhibit elevated dielectric constants (ϵ), which substantially attenuate Coulombic interactions between ionic species. As described by Coulomb's law ($F = k(q_1q_2)/\epsilon r^2$), the increased dielectric constant diminishes interionic repulsive forces, thus promoting charge transfer efficiency. Moreover, high-polarity solvents demonstrate intensified intermolecular interactions, including hydrogen bonding and dipole-dipole interactions, which collectively contribute to the stabilization of the transition state in charge transfer complexes.

To further clarify the correlation between solvent polarity and the CT in dimer, a correlation analysis was performed on the data in [Table 1](#), as shown in [Supplementary Table S1](#). The total level of CT between fragments 1 and 3 was notably dependent on the polarity of the solvent. A higher solvent polarity corresponded to a greater amount of CT. Furthermore, the level of charge transfer between fragments 1 and 3 was highly correlated with the overall CT in the dimer. The correlation coefficient was 1, indicating that almost all of the CT in Chl dimer was provided by fragments 1 and 3. This is consistent with the existing conclusion that the porphyrin ring

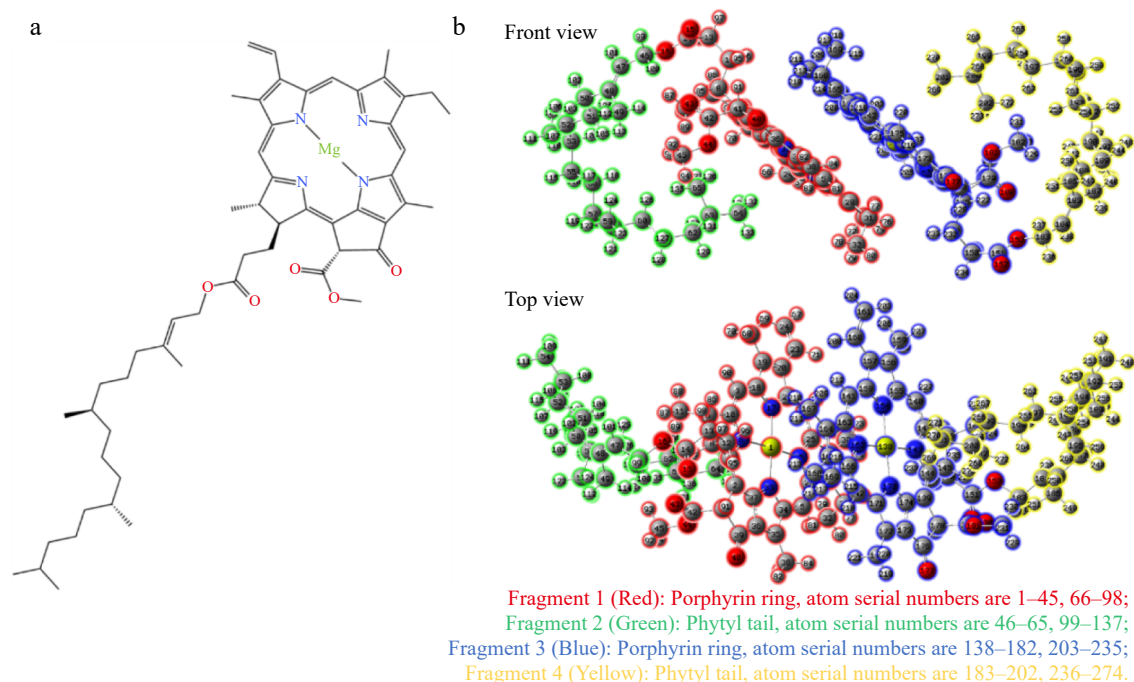


Fig. 1 (a) Structure of Chl *a* and (b) selected fragments of Chl 'face-to-face' dimer.

Table 1. The amount of charge transfer between different fragments of Chl dimer in different concentrations of ethanol solvents.

Proportion of ethanol	10%	20%	30%	40%	50%	60%	70%	80%	90%	100%
Net 1→2:	0.00003	0.00003	0.00003	0.00003	0.00003	0.00003	0.00003	0.00003	0.00003	0.00003
Net 1→3:	0.95285	0.95251	0.9521	0.95158	0.95097	0.95015	0.94901	0.94746	0.9451	0.94029
Net 1→4:	0.00072	0.00072	0.00072	0.00072	0.00072	0.00072	0.00072	0.00072	0.00073	0.00072
Net 2→3:	0.00136	0.00136	0.00136	0.00136	0.00135	0.00135	0.00135	0.00135	0.00135	0.00135
Net 2→4:	0	0	0	0	0	0	0	0	0	0
Net 3→4:	−0.00007	−0.00007	−0.00007	−0.00007	−0.00007	−0.00007	−0.00007	−0.00007	−0.00007	−0.00007
Total	0.95503	0.95469	0.95428	0.95376	0.95314	0.95232	0.95118	0.94963	0.94728	0.94246

Fragment 1: porphyrin ring, atom serial numbers are 1–45, 66–98; 2: phytol tail, atom serial numbers are 46–65, 99–137; 3: porphyrin ring, atom serial numbers are 138–182, 203–235; 4: phytol tail, atom serial numbers are 183–202, 236–274.

structure of Chl enables it to efficiently harvest light and transfer electrons in photosynthesis^[26]. The porphyrin ring has the ability to transfer charges due to its highly conjugated structure, while the phytol chain does not have this ability. The experimental results unequivocally demonstrated that solvent polarity exerted a significant influence on CT interactions, with strongly polar solvents being particularly conducive to the formation of robust CT complexes.

To further substantiate the correlation between increased solvent polarity and heightened CT interaction, fluorescence detection was conducted on Chl samples in various polar solvents, as depicted in Fig. 2a. This observation suggests that as the solvent polarity heightened, there was a corresponding increase in fluorescence quenching. This quenching meant that there was aggregation between Chl molecules^[27]. It also shows that strong polarity induced Chl aggregation^[10]. The fluorescence quenching produced a sharp increase in the range of 50%–70% ethanol proportion, which was similar to the result of Yasuda^[10]. This indicates that there was a critical threshold of solvent polarity at which the aggregation of Chl was notably enhanced within this range. It appears that the CT phenomenon was accompanied by Chl aggregation, which suggests that the polar solvent enhanced the CT of the system while inducing Chl aggregation^[28]. It is worth mentioning that in Yasuda's research, water was added to the ethanol solution of Chl to prepare Chl solutions with different ethanol concentrations^[10]. In this scenario, the hydrophobic nature of Chl means that the introduction of water into the ethanol solution will promote Chl aggregation. As a result of varying water proportions in the solvents, different Chl aggregates were formed. Consequently, three distinct forms of Chl were identified in the solvents with ethanol proportions ranging from 10% to 100% in their research. However, a similar phenomenon did not occur in this study, and the stability of Chl in solvents with different ethanol concentrations was also different from their result. The reason for this was that a different method of preparing the Chl solution was attempted in order to bring the samples into states more similar to Chl products. In the food

industry, the agitation during transport and extended storage will eventually lead to the formation of stable Chl aggregates in the solvents, thereby diminishing the differences in Chl aggregations induced by the variation in Chl solubility between water and ethanol at the initial stage of processing. The weak interaction within Chl aggregates made them highly susceptible to depolymerization, particularly due to agitation during transport. Consequently, in this study, a small amount of high-concentration Chl ethanol solution was added to a large amount of ethanol-water solvent when preparing Chl samples. This approach aimed to ensure that Chl aggregates existed in more uniform forms across different concentrations of ethanol solvents.

Figure 2b shows the conductivity of Chl samples in different polar environments. Overall, conductivity rises with increased polarity. The conductivity was closely linked to CT and essentially mirrored the electron transfer process^[29]. When the CT interaction is more active, the conductivity of sample will be higher. Therefore, Fig. 2b means that Chl had aggregated, and the increase in conductivity was due to the aggregation of Chl induced by the polar environment, which enhanced the CT interaction.

The effect of solvent polarity on stability of Chl

Although the previous research discussed many methods to enhance Chl stability through Chl aggregation, the specific forces involved in microscopic interactions, especially the unique CT interactions within Chl aggregates, were not further analyzed in relation to Chl stability^[11,12,30–32]. This study aimed to elucidate the factors governing the strength of CT interactions, with the objective of leveraging CT regulation as a strategy to enhance Chl stability. The findings demonstrate that increased solvent polarity positively correlates with the enhancement of CT interactions. Furthermore, we systematically investigated the relationship between solvent polarity and Chl stability, providing mechanistic insights into this stabilization phenomenon. Since light was the most significant factor affecting the stability of Chl, light treatment was used to

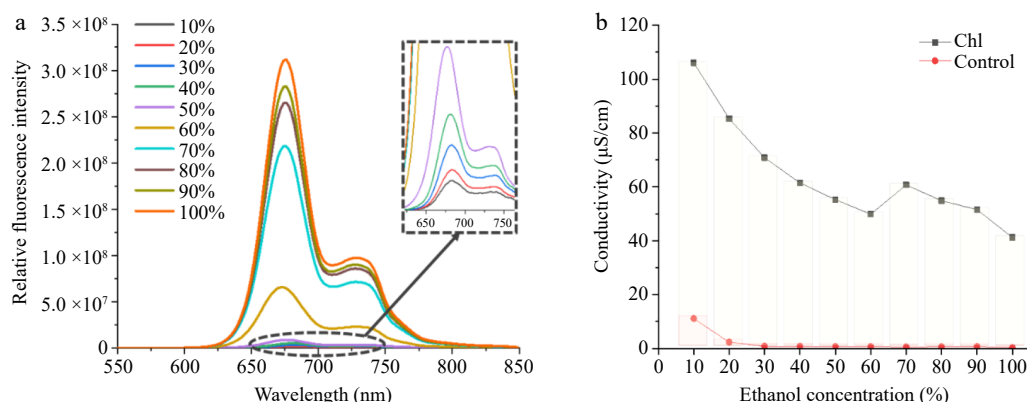


Fig. 2 Proof of Chl aggregation. (a) Chl fluorescence emission spectra in solvents of different polarities. (b) Chl conductivity in ethanol solvents of different concentrations.

interfere with the stability of Chl^[12]. As shown in Fig. 3a, it is revealed that the color of the samples remained better in ethanol solvents with a proportion of 10%–50%, while the green color in 60%–100% ethanol solvents noticeably faded, particularly in the 70%–90% range. This suggests that in a highly polar environment, the interaction of CT was stronger, leading to better stability of Chl.

Corresponding to Fig. 3a, the Chl content was measured, as shown in Fig. 3b. The relative trend of the decrease of Chl content in each group of samples remained the same on 4 d and 8 d. On the whole, the samples were divided into 3 categories according to the degradation rate: ethanol proportion was between 10%–40%: the solvent was more polar, and the Chl stability was stronger, which was consistent with previous studies^[10,33]; ethanol proportion was 50% or 100%: Chl stability transition zone; ethanol proportion was between 60%–90%: the solvent polarity was weak and the Chl stability was poor. Among the findings, on the fourth day, Chl exhibited the strongest stability in 20% ethanol, with a retention rate of 88.03%, while on the eighth day, Chl showed the strongest stability in 30% ethanol, with a retention rate of 69.51%. Conversely, on the fourth day, Chl demonstrated the worst stability in 70% ethanol, with a retention rate of 41.32%, and on the eighth day, Chl showed the worst stability in 80% ethanol, with a retention rate of 22.97%. Specifically, Chl retention in the high-polarity treatment group showed a substantial increase, reaching 213.04% and 302.61% of the low-polarity group values on day four and day eight, respectively. Thus, a higher-polarity solvent environment was found to promote Chl stability. These results indicate a positive correlation between CT interaction strength and Chl stability. However, the

underlying mechanism of Chl stabilization was not directly attributed to solvent polarity effects but rather to the formation of Chl molecular aggregates. Consequently, the stability analysis presented in this study fundamentally relies on the established role of Chl aggregation as the primary stabilizing factor.

The effect of phytyl tail on CT

Although previous studies have established that CT in Chl dimers primarily occurs between porphyrin rings, with negligible contribution from the phytyl tail, the steric and hydrophobic effects of this moiety nevertheless constitute a non-negligible factor in stabilizing Chl aggregates. Beyond solvent polarity considerations, the phytyl chain represents the most probable secondary modulator of CT characteristics. This structural component warrants particular attention, as it plays a decisive role in accounting for the fine variations in CT interactions observed among different Chl aggregate configurations. In addition, the phytyl tail was an important fragment other than the porphyrin ring of Chl, playing an important role in the interaction between Chl and protein and other macromolecules in plants^[9,34,35]. Therefore, it was necessary to explain the influence of phytyl on CT. As distance is one of the primary factors affecting CT interaction, two Chl dimer models with varying porphyrin ring spacings were chosen to investigate the effect of the phytyl tail on CT, as shown in Fig. 4. Figure 4a to c are the HOMO-LUMO orbital diagrams after removing the phytyl in turn, based on the configuration of Chl 'sandwich' dimer in ethanol. The HOMO-LUMO orbitals showed obvious CT characteristics. The alterations in the electronic motion regions observed in the HOMO-LUMO orbitals were deemed to provide a good approximation for reactivity. This shows that CT

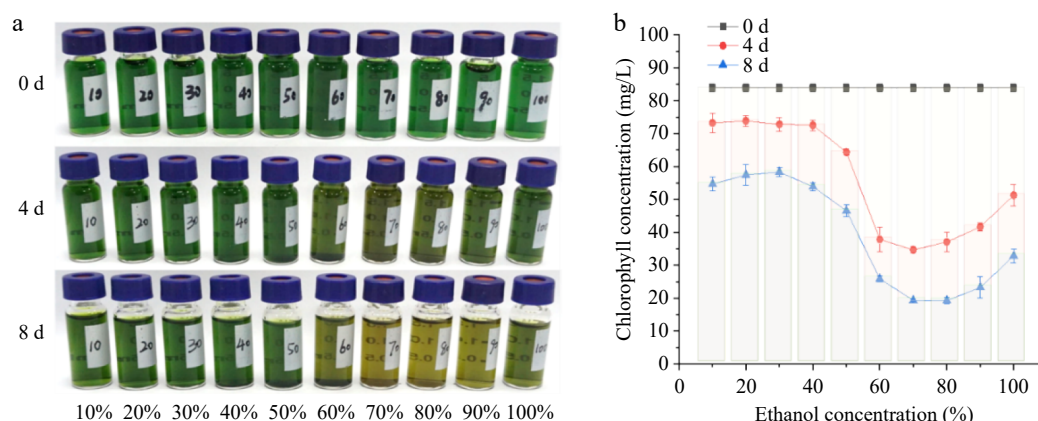


Fig. 3 Proofs of the improvement of Chl stability by polar solvent. (a) Green stability of Chl in different concentrations of ethanol during storage. (b) Changes in the concentration of Chl in different concentrations of ethanol solvents during storage.

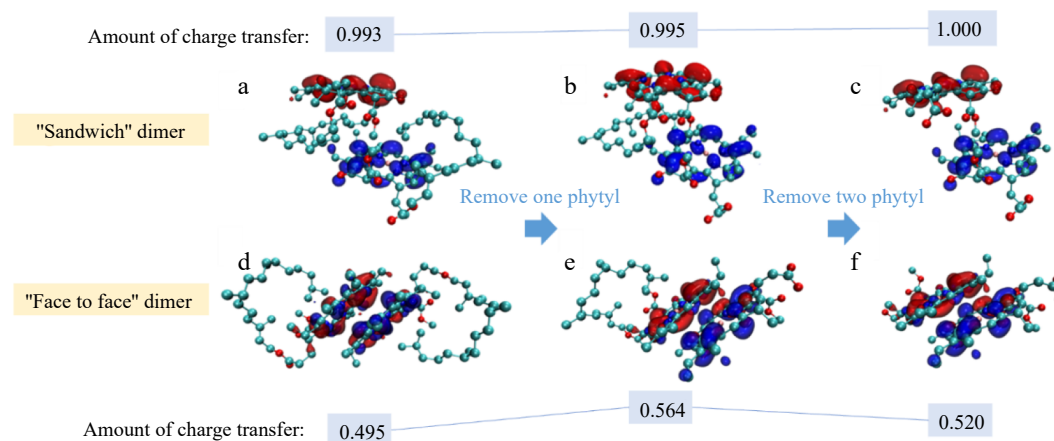


Fig. 4 The relationship between the configuration of dimers in ethanol and the amount of charge transfer between porphyrin rings (red: HOMO; blue: LUMO).

interaction was easy to obtain in the models with the configuration of the Chl 'sandwich' dimer series. The change of the HOMO-LUMO orbitals can be used to study the change of the most easily available CT interaction in the aggregate. The presence or absence of the phytyl tail had no obvious influence on the overall HOMO-LUMO orbital distribution in the Chl 'sandwich' dimer. In Fig. 4d–f, models of Chl 'face-to-face' dimers with relatively closer porphyrin ring spacing were used. The absence of the phytyl group led to significant changes in the HOMO-LUMO orbitals of the Chl dimer, revealing more pronounced CT characteristics.

To quantify the effect of phytyl on CT more accurately, the IFCT analysis of the CT was carried out. Before IFCT analysis, an excited state that can reflect the characteristics of the CT of the HOMO-LUMO orbital must be selected first so as to conduct a comparison within the groups. The screening results are shown in [Supplementary Table S2](#), and the first five excited states of the six configurations were used as the screening range. When the Chl 'sandwich' series reached S_5 , the hole-electron contribution in the HOMO-LUMO orbital was the most prominent, which means that the CT interaction of S_5 was the most obvious. When the Chl 'face-to-face' series reached S_3 , the effect of CT in the HOMO-LUMO orbital was the most obvious. Therefore, in the next step of the study, S_5 of the Chl 'sandwich' series and S_3 of the Chl 'face-to-face' series were used as models to study the impact of the phytyl on CT.

As shown in Fig. 4, as the phytyl tails were gradually removed, the CT amount of Chl 'sandwich' dimer increased, while the CT amount increased first and then decreased in Chl 'face-to-face' dimer. The alterations in CT resulting from the removal of the phytyl tails fully illustrate the impact of phytyl on the CT interaction within the Chl aggregates. Table 2 shows the amount of charge movement between phytyl tails and porphyrin rings in different configurations, also showing that phytyl tails affected the CT between porphyrin rings. It should be noted that the CT occurring in the Chl dimer primarily involves the transfer of charges between individual monomer molecules. In contrast, the transfer of charges between the phytyl tail and the porphyrin ring within a single molecule represents a local excitation, which does not currently enable intermolecular charge transfer. Under these circumstances, the phytyl group disrupts the charge transfer interaction between the porphyrin rings of the two molecules by inducing a charge movement within the porphyrin ring. This mechanism facilitates the manifestation of the impact of the phytyl tail on charge transfer. The total amount of charge transfer in Table 2 is very similar to the change of the charge transfer amount shown in Fig. 4, which is consistent with the described above. This indicates that the primary factor contributing to the variation in the strength of charge transfer interactions within the aggregates was the alteration in the charge transfer capability of the aggregates themselves resulting from a configuration change, which in turn arose from the removal of phytyl tails.

Combining Fig. 4 and Table 2, it was analyzed that the phytyl tail interfered with the CT in the Chl dimer. When the porphyrin rings were far apart from each other, the presence of the phytyl tail hindered the charge transfer. On the other hand, when the porphyrin rings were in close proximity, the phytyl moiety restricted a portion of the charge on the outer surface of the porphyrin ring due to its involvement in the charge transfer between the

fragments. Therefore, the amount of charge transfer of Fig. 4d was less than that of Fig. 4f. However, when there was only one phytyl tail as in Fig. 4e, when the electrons released by the monomer without phytyl tail and move away from porphyrin rings, part of them were tending to be attracted by the phytyl on the opposite monomer due to the attraction of phytyl to charge. Consequently, the electrons located at a distance from the porphyrin ring exhibited a propensity to migrate towards the adjacent porphyrin ring, thereby reinforcing the charge transfer between the porphyrin rings, as shown in Fig. 4e.

Conclusions

This study conducted an analysis of the factors influencing CT in Chl aggregates and their relationship with aggregate stability. The study demonstrated that solvent polarity was a significant factor influencing charge transfer, with a stronger solvent polarity leading to a more robust charge transfer interaction. In a polar environment, the stability of Chl was notably enhanced, reaching a relatively stable state with a high level of stability in a solution containing 10–40% ethanol. On the fourth and eighth day under light treatment, the Chl retention in the high polarity group reached 213.04% and 302.61% of the low polarity group, respectively. During Chl aggregation, the influence of different solvent polarities led to varying strengths of CT interactions between the Chl molecules, thereby promoting the formation of stable aggregates with diverse configurations. In addition to solvent polarity, phytyl was also a key factor affecting the CT of Chl aggregates. Its influence on the configuration of Chl aggregates led to changes in the charge transfer of the aggregates. Once the aggregate configuration was stabilized, the phytyl tails continued to be involved in the modulation of the charge transfer interactions between the porphyrin rings. In general, the higher polar environment was conducive to the use of stronger CT interaction to promote the Chl aggregation to make Chl more stable. Compared with vdW forces and electrostatic forces, CT interactions have more unique characteristics and are more likely to be artificially regulated. The results of this study mean that in the future, it may be possible to induce Chl aggregation through the regulation of CT by electric or magnetic fields, thereby improving Chl stability. This will open new avenues for the development of more physical methods to protect the stability of natural pigments.

Author contributions

The authors confirm their contributions to the paper as follows: conceptualization: Li F, Zhang Y, methodology: Li F, Yang Z, Shen S, Ibrahim AN, Wang Z; validation: Yang Z, Shen S; investigation: Li F, Yang Z, Shen S, Ibrahim AN; data curation: Yang Z, Zhang Y; software: Li F, Wang Z; formal analysis, writing - original draft: Li F; writing - review & editing: Li F, Zhang Y; visualization: Yang Z; resources, supervision, project administration, funding acquisition: Zhang Y. All authors reviewed the results and approved the final version of the manuscript.

Data availability

The authors confirm that the data supporting the findings of this study are available within the article and its supplementary materials.

Acknowledgments

This work was supported by the Xinjiang Central Guidance for Local Science and Technology Development Funds Project (Grant No. ZYD2024QY05), the Hainan Provincial Natural Science

Table 2. The amount of charge transfer in different aggregate models.

	A	B	C	D	E	F
Porphyrin ring → Phytyl tail	0.00192	0.00216	–	–0.00004	0.00035	–
Porphyrin ring ↔ Phytyl tail	0.00410	0.00440	–	0.00080	0.00035	–
Total charge transfer	0.99741	0.9996	1	0.49531	0.56446	0.52039

Foundation of China (Grant No. 323CXTD381) and the National Key R&D Program of China (Grant No. 2024YFD2101101), within program Grant No. 2024YFD2101100.

Conflict of interest

The authors declare that they have no conflict of interest.

Supplementary information accompanies this paper at (<https://www.maxapress.com/article/doi/10.48130/fia-0025-0039>)

Dates

Received 21 January 2025; Revised 30 April 2025; Accepted 8 May 2025; Published online 29 October 2025

References

1. Albuquerque BR, Oliveira MBPP, Barros L, Ferreira ICFR. 2021. Could fruits be a reliable source of food colorants? Pros and cons of these natural additives. *Critical Reviews in Food Science and Nutrition* 61:805–35
2. Viera I, Pérez-Gálvez A, Roca M. 2019. Green natural colorants. *Molecules* 24:154
3. Li Y, Lu F, Wang X, Hu X, Liao X, et al. 2021. Biological transformation of chlorophyll-rich spinach (*Spinacia oleracea* L.) extracts under in vitro gastrointestinal digestion and colonic fermentation. *Food Research International* 139:109941
4. Li Y, Cui Y, Hu X, Liao X, Zhang Y. 2019. Chlorophyll supplementation in early life prevents diet-induced obesity and modulates gut microbiota in mice. *Molecular Nutrition & Food Research* 63:1801219
5. Li Y, Cui Y, Lu F, Wang X, Liao X, et al. 2019. Beneficial effects of a chlorophyll-rich spinach extract supplementation on prevention of obesity and modulation of gut microbiota in high-fat diet-fed mice. *Journal of Functional Foods* 60:103436
6. Fiedor L, Zbyradowski M, Pilch M. 2019. Tetrapyrrole pigments of photosynthetic antennae and reaction centers of higher plants: Structures, biophysics, functions, biochemistry, mechanisms of regulation, applications. In *Advances in Botanical Research*, ed. Grimm B. vol. 90. Cambridge, Massachusetts, USA: Academic Press. pp. 1–33 doi: 10.1016/bs.abr.2019.04.001
7. Pérez-Gálvez A, Viera I, Roca M. 2020. Carotenoids and chlorophylls as antioxidants. *Antioxidants* 9:505
8. Taniguchi M, Lindsey JS. 2021. Absorption and fluorescence spectral database of chlorophylls and analogues. *Photochemistry and Photobiology* 97:136–65
9. Cao J, Li F, Li Y, Chen H, Liao X, et al. 2020. Hydrophobic interaction driving the binding of soybean protein isolate and chlorophyll: Improvements to the thermal stability of chlorophyll. *Food Hydrocolloids* 113:106465
10. Yasuda M, Oda K, Ueda T, Tabata M. 2019. Physico-chemical chlorophyll-a species in aqueous alcohol solutions determine the rate of its discoloration under UV light. *Food Chemistry* 277:463–70
11. Li F, Zhou L, Cao J, Wang Z, Liao X, et al. 2022. Aggregation induced by the synergy of sodium chloride and high-pressure improves chlorophyll stability. *Food Chemistry* 366:130577
12. Li F, Cao J, Wang Z, Liao X, Hu X, et al. 2022. Dual aggregation in ground state and ground-excited state induced by high concentrations contributes to chlorophyll stability. *Food Chemistry* 383:132447
13. Wang X, Pan M, Shi Z, Yu D, Huang F. 2021. Protein nanobarrel for integrating chlorophyll a molecules and its photochemical performance. *ACS Applied Bio Materials* 4:399–405
14. Wang X, Liu C, Shi Z, Pan M, Yu D. 2020. Protein-encapsulated chlorophyll a molecules for biological solar cells. *Materials & Design* 195:108983
15. Naresh M, Srivishnu KS, Krishna YR, Mrinalini M, Prasanthkumar S. 2021. Light stimulated donor-acceptor forms charge transfer complex in chlorinated solvents. *Journal of Chemical Sciences* 133:70
16. Panigrahi S, Misra PK. 2016. The effect of solvent on electronic absorption bands of some Benzylideneanilines. *Journal of Molecular Liquids* 224:53–61
17. Frisch MJ, Trucks GW, Schlegel HB, Scuseria GE, Robb MA, et al. 2016. *GAUSSIAN16. Revision C.01*. Gaussian Inc., Wallingford, CT, USA
18. Stephens PJ, Devlin FJ, Chabalowski CF, Frisch MJ. 1994. Ab initio calculation of vibrational absorption and circular dichroism spectra using density functional force fields. *The Journal of Physical Chemistry* 98:11623–27
19. Lu T, Chen F. 2013. Revealing the nature of intermolecular interaction and configurational preference of the nonpolar molecular dimers (H₂)₂, (N₂)₂, and (H₂)(N₂). *Journal of Molecular Modeling* 19:5387–95
20. Zhao Y, Truhlar DG. 2008. The M06 suite of density functionals for main group thermochemistry, thermochemical kinetics, noncovalent interactions, excited states, and transition elements: two new functionals and systematic testing of four M06 functionals and 12 other functionals. *Theoretical Chemistry Accounts* 119:525
21. Yanai T, Tew DP, Handy NC. 2004. A new hybrid exchange–correlation functional using the Coulomb-attenuating method (CAM-B3LYP). *Chemical Physics Letters* 393:51–57
22. Lu T, Chen F. 2012. Multiwfn: a multifunctional wavefunction analyzer. *Journal of Computational Chemistry* 33:580–92
23. Toprak Aktas E, Yildiz H. 2011. Effects of electropulsolysis treatment on chlorophyll and carotenoid extraction yield from spinach and tomato. *Journal of Food Engineering* 106:339–46
24. Merzlyak MN, Melø TB, Naqvi KR. 2008. Effect of anthocyanins, carotenoids, and flavonols on chlorophyll fluorescence excitation spectra in apple fruit: signature analysis, assessment, modelling, and relevance to photoprotection. *Journal of Experimental Botany* 59:349–59
25. Lee KJ, Xiao Y, Kim ES, Mathevet F, Mager L, et al. 2019. Donor–Acceptor Distance-Dependent Charge Transfer Dynamics Controlled by Metamaterial Structures. *ACS Photonics* 6:2649–54
26. Wang W, Yu LJ, Xu C, Tomizaki T, Zhao S, et al. 2019. Structural basis for blue-green light harvesting and energy dissipation in diatoms. *Science* 363:eaav0365
27. Qu F, Gong N, Wang S, Gao Y, Sun C, et al. 2020. Effect of pH on fluorescence and absorption of aggregates of chlorophyll a and carotenoids. *Dyes and Pigments* 173:107975
28. Buscemi G, Vona D, Trotta M, Milano F, Farinola GM. 2022. Chlorophylls as molecular semiconductors: introduction and state of art. *Advanced Materials Technologies* 7:2100245
29. Burian M, Rigodanza F, Demitri N, Dordević L, Marchesan S, et al. 2018. Inter-Backbone Charge Transfer as Prerequisite for Long-Range Conductivity in Perylene Bisimide Hydrogels. *ACS Nano* 12:5800–06
30. Li F, Yang Z, Shen S, Wang Z, Zhang Y. 2023. Ternary synergistic aggregation of chlorophyll/Soy protein isolate improves chlorophyll stability. *Food Hydrocolloids* 140:108662
31. Cao J, Li Y, Li F, Liao X, Hu X, et al. 2022. Effect of high hydrostatic pressure on chlorophyll/soybean protein isolate interaction and the mixtures properties. *Food Hydrocolloids* 128:107555
32. Wang L, Li W, Li F, Zeng M. 2023. Mechanism of Enhancing Chlorophyll Photostability through Light-Induced Chlorophyll/Phycocyanin Aggregation. *Journal of Agricultural and Food Chemistry* 71:19010–19
33. Shen SC, Hsu HY, Huang CN, Wu JSB. 2010. Color loss in ethanolic solutions of chlorophyll a. *Journal of Agricultural and Food Chemistry* 58:8056–60
34. Bednarczyk D, Tor-Cohen C, Das PK, Noy D. 2021. Direct assembly in aqueous solutions of stable chlorophyllide complexes with type II water-soluble chlorophyll proteins. *Photochemistry and Photobiology* 97:732–38
35. Palm DM, Agostini A, Pohland AC, Werwie M, Jaenicke E, et al. 2019. Stability of water-soluble chlorophyll protein (WSCP) depends on phytol conformation. *ACS Omega* 4:7971–79



Copyright: © 2025 by the author(s). Published by Maximum Academic Press on behalf of China Agricultural University, Zhejiang University and Shenyang Agricultural University. This article is an open access article distributed under Creative Commons Attribution License (CC BY 4.0), visit <https://creativecommons.org/licenses/by/4.0/>.